Proc. Natl. Acad. Sci. USA
Vol. 92, pp. 954–958, February 1995
Neurobiology

Superoxide dismutase is an abundant component in cell bodies, dendrites, and axons of motor neurons and in a subset of other neurons

CARLOS A. PARDO*†, ZUOSHANG XU‡, DAVID R. BORCHELT*†, DONALD L. PRICE*†§, SANGRAM S. SISODIA*†, AND DON W. CLEVELAND‡§

*Neuropathology Laboratory and Departments of †Pathology, ‡Biological Chemistry, and §Neuroscience, Johns Hopkins University School of Medicine, Baltimore, MD 21205

Communicated by Marc W. Kirschner, Harvard Medical School, Boston, MA, October 21, 1994

ABSTRACT **Mutation in superoxide dismutase 1 (SOD1), a Cu/Zn enzyme that removes oxygen radicals and protects against oxidative injury, has been implicated in some cases of familial amyotrophic lateral sclerosis (FALS). As a first approach to examining the mechanism(s) through which these mutations cause specific degeneration of motor neurons, we have used immunocytochemistry to identify the distribution of SOD1 in populations of cells in the peripheral and central nervous systems. In the spinal cord, intense SOD1 immunoreactivity was present in motor neurons, interneurons, and substantia gelatinosa. In motor neurons, SOD1 immunoreactivity was abundant in perikarya, dendrites, and axons; most of this activity appeared to be free in the cytoplasm, although a portion was associated with membranous vesicles, presumably peroxisomes. Since a variety of central nervous system neurons, including pyramidal cells in cerebral cortex and neurons of the CA3 and CA4 sectors of the hippocampus, showed high immunoreactivity but are unaffected in ALS, the apparent abundance of SOD1 does not predict vulnerability of neurons to mutations in SOD1. Rather, SOD1 accumulates in many neuronal populations but is particularly abundant in motor neurons. Consistent with recent studies of FALS-linked SOD1 mutations *in vitro* and in transgenic mice, our findings offer further support for the view that the mutations confer a gain of adverse function. In this view, high, rather than limiting, levels of SOD1 may place motor neurons selectively at risk in FALS.**

Part of the free-radical scavenger system, superoxide dismutases (SODs; EC 1.15.1.1) include SOD1, a cystosolic Cu/Zn enzyme; SOD2, a Mn-containing mitochondrial matrix SOD; and SOD3, an extracellular form of Cu/Zn SOD (1). These metalloenzymes catalyze the dismutation of superoxide anions (O_2^-), yielding H_2O_2 and O_2; subsequent removal of H_2O_2 is facilitated by catalase and glutathione peroxidase (2). Thus, SOD activity can protect against oxidative stress produced by oxygen radicals and may represent a first line of defense against oxidative damage mediated by oxygen radicals (1, 2).

SODs are present in the central and peripheral nervous systems, but the cellular and intracellular distributions of SOD1 in neuronal populations are not well defined. Biochemical assays of SOD1 activity have not localized enzymatic activities to specific cells in the brain (3, 4), and *in situ* hybridization and immunocytochemical studies have focused only on selected areas of the nervous system in either control (5–8) or diseased (9, 10) brain.

It has been hypothesized that alterations in antioxidant systems, including SOD1, are implicated in neurodegenerative diseases (5, 11–15). In some cases of familial amyotrophic lateral sclerosis (FALS), mutations in SOD1 have been linked to disease (16–18), and at least two of these mutations can cause motor neuron disease when expressed in transgenic mice (ref. 19; unpublished observations). However, the mechanism(s) responsible for selective vulnerability to degeneration of motor neurons in FALS-linked SOD1 mutations is unknown. To identify events that lead to motor neuron death, it is critical to define the cellular distributions of SOD1 in the peripheral and central nervous systems. To this end, we have used protein blotting and immunocytochemistry at both light and electron microscopic levels to localize SOD1 in the mouse, nonhuman primate, and human nervous systems.

MATERIALS AND METHODS

Generation and Characterization of anti-SOD1 Antibody. A pentadecapeptide (CYDDLGDGGNEESTK) of which the C-terminal 13 amino acids correspond to residues 125–137 of mouse and human SOD1 was crosslinked to keyhole limpet hemocyanin (Pierce), emulsified in Freund's adjuvant, and used to immunize rabbits, as described (20). Rabbit serum was subjected to affinity purification by binding to the oligopeptide coupled to CNBr-activated Sepharose 4B (Pharmacia). Bound antibody was eluted with 0.1 M sodium citrate, quickly neutralized, brought to 0.5% bovine serum albumin, and stored in aliquots at −80°C. To characterize the antibody, purified human SOD1 (Sigma) or proteins extracts from mouse neuroblastoma (N2a) cells and mouse and human nervous tissues were analyzed by immunoblotting. Human and mouse tissues were homogenized with a Brinkmann Polytron at 20% (wt/vol) in 25 mM sodium phosphate, pH 7.2/1 mM EGTA/1% SDS. Human tissue (frontal and motor cortex, hippocampus, and spinal cord) were obtained at autopsy from a patient who died of a non-neurological disease. Protein concentrations were determined by a bicinchoninic acid assay (Pierce), and 100-μg samples of protein were fractionated by electrophoresis in SDS/15% polyacrylamide gels (21) and transferred to nitrocellulose filters (20). Filters were then incubated with the affinity-purified antibody (at 1:2000 dilution) followed by ^{125}I-labeled protein A (Amersham) and bound antibody was detected with x-ray film (Eastman Kodak).

Tissue Preparation. Mice (C57B6/C F_1) between the ages of 2 and 4 months (20–25 g) were anesthetized with intraperitoneal injections of chloral hydrate and perfused with phosphate-buffered saline (pH 7.4), followed by fixation with 4% paraformaldehyde in 0.1 M phosphate buffer. Brains and spinal cords were postfixed for 1 hr in the same fixative, and cryoprotected in 30% sucrose in 0.1 M phosphate buffer for 24 hr. A series of horizontal and coronal sections of brain and of cervical, thoracic, and lumbosacral spinal cord were cut (40 μm) on a freezing microtome. After perfusions with phosphate-buffered saline and fixation with 4% paraformaldehyde in 0.1 M phosphate buffer, brain and spinal cord were also

The publication costs of this article were defrayed in part by page charge payment. This article must therefore be hereby marked "*advertisement*" in accordance with 18 U.S.C. §1734 solely to indicate this fact.

Abbreviations: SOD, superoxide dismutase; FALS, familial amyotrophic lateral sclerosis.

obtained from two young baboons and an adult rhesus monkey. In addition, brain and spinal cord were obtained at autopsy from two humans who died of non-neurological disorders, and temporal cortex was also obtained from two individuals who underwent surgery for epilepsy. These human tissues were dissected and fixed in 4% paraformaldehyde in 0.1 M phosphate buffer for 48 hr, cryoprotected in 30% sucrose in 0.1 M phosphate buffer for 24 hr, and frozen. All tissues were cut on a freezing microtome.

Histology and Immunocytochemistry. For all evaluations of SOD1 immunoreactivity, an initial set of sections was stained with cresyl violet to define cytoarchitectural landmarks. For immunocytochemistry, a second series of sections was rinsed in Tris-buffered saline (TBS: 50 mM Tris·HCl, pH 7.2/140 mM NaCl) and incubated for 1 hr in a blocking solution (5% normal goat serum/0.25% Triton X-100/TBS) and then for 48 hr at 4°C with an anti-SOD1 antibody (pAb-m/h-SOD1) diluted 1:1000 in 3% normal goat serum/TBS. Sections were washed in TBS and incubated with a biotinylated secondary antibody and then with horseradish peroxidase covalently linked to streptavidin. Reaction product was developed by incubation in 0.03% diaminobenzidine/0.01% H_2O_2/TBS. Sections were rinsed in TBS, mounted onto gelatin-coated slides, dehydrated in a series of graded ethanol solutions followed by xylene, and then coverslipped. A third series of sections was incubated with primary antibody preadsorbed to the immunizing peptide. A fourth series of sections was incubated with nonimmune rabbit serum.

Immunoelectron Microscopy. For immunoelectron microscopy, mice were perfused with 4% paraformaldehyde and 0.1% glutaraldehyde in 0.1 M phosphate buffer (pH 7.2) and postfixed in the same fixative for 30 min. Monkey and baboon tissue was postfixed in 4% paraformaldehyde and 0.1% glutaraldehyde in 0.1 M phosphate buffer for 1 hr. Brain tissue and spinal cords were cut (50 μm) on a vibrating microtome, pretreated with 0.1 M glycine (pH 7.2), and processed for immunocytochemistry according to a modified protocol for silver-enhanced immunogold labeling (22). Sections from cervical and lumbar spinal cord, cerebral cortex, hippocampus, and striatum were selected for immuno-ultrastructural analysis. Semi-thin and thin sections were cut and counterstained with lead citrate and uranyl acetate and examined in the electron microscope.

RESULTS

Characterization of SOD1 Antibody. To produce an antibody that could specifically detect mammalian SOD1, we synthesized a 15-amino acid peptide corresponding to residues 125–137 of human and mouse SOD1 (23–25). One rabbit produced a high-titer response. After affinity purification, this antibody (pAb-m/h-SOD1) revealed strong immunoreactivity with, and specificity for, the 16-kDa mouse SOD1 polypeptide on immunoblots of whole cell extracts of the mouse neuroblastoma N2a cell line (Fig. 1*B*, lane N2a). Specific immunoreactivity was also seen with purified human SOD1 (Fig. 1*B*, lane hSOD1) or human SOD1 expressed in N2a cells stably transfected with a plasmid (pHGSOD.SVneo) containing the human SOD1 gene (26) [Fig. 1*B*, lane N2a (hSOD1)]. Similarly, in tissue extracts from mouse (Fig. 1*C*) or human nervous tissue (Fig. 1 *D* and *E*), the antibody bound specifically to a polypeptide of the size expected for SOD1. By comparison of the relative intensity of the immunoblot signals generated by 200 ng of purified human erythrocyte SOD1 and the SOD1 in 100 μg of murine and human nervous tissues, we estimated that SOD1 comprised 1–2% of the total detergent-soluble proteins in each sample.

Localization of SOD1 in the Mammalian Nervous System. Sections from spinal cord, cerebral cortex, and subcortical regions from mouse, monkey, baboon, and human brains were immunostained with the antibody against SOD1 (pAb-m/h-SOD1). To obtain optimal fixation and to minimize complications arising from postmortem delay in tissue recovery, the human tissues examined were obtained from short-postmortem-delay autopsies or surgical resections and were fixed immediately following tissue removal. SOD1 immunoreactivity was primarily identified in neurons. In spinal cord, SOD1 immunoreactivity was readily discernible in motor neurons, interneurons, and sensory neurons. Throughout all segments of the spinal cord, SOD1 immunoreactivity was observed in motor neurons, small neurons, some astrocytes in white matter, and ependymal cells in the central canal. The most intense staining was found in the cell bodies of large motor neurons from mouse (Fig. 2 *A* and *C*) and human (Fig. 2 *D–F*). This staining was specific, since preincubation of the antibody with the immunizing peptide (100 μg/ml) completely eliminated reactivity (Fig. 2*B*). Higher magnification revealed a predominantly punctate (particulate) pattern, readily visualized throughout the perikarya and proximal dendrites (Fig. 2 *C–F*). Similar distributions of SOD1 immunoreactivity were observed in mice, nonhuman primates, and humans. Some axons in the spinal cord showed SOD1 immunoreactivity. The enzyme was most abundant in terminals of neurons of the dorsal root ganglia projecting to the substantia gelatinosa

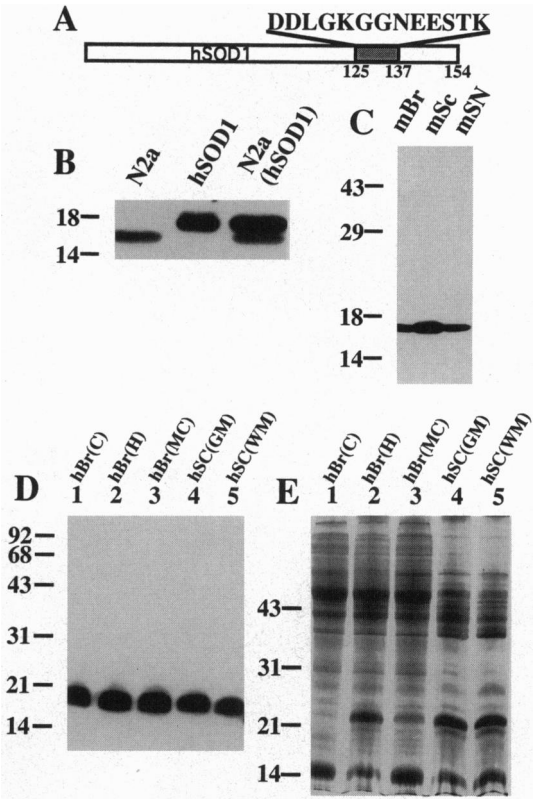

FIG. 1. Characterization of pAb-m/h-SOD1, a polyclonal antibody to mammalian SOD1. (*A*) Diagram of human (h) SOD1 protein highlighting the oligopeptide used to produce antibody pAb-m/h-SOD1. (*B*) Specificity of pAb-m/h-SOD1 on immunoblots of whole cell extracts from N2a cells (lane N2a) or N2a cells stably transfected to express human SOD1 [lane N2a (hSOD1)]. Immunoblot of purified human SOD1 (lane hSOD1) is shown for comparison. Molecular mass markers are in kilodaltons. (*C*) Specificity of pAb-m/h-SOD1 on immunoblots of 100 μg of protein in detergent-soluble extracts of mouse brain (lane mBr), mouse spinal cord (lane mSc), and mouse sciatic nerve (lane mSN). (*D* and *E*) Specificity of pAb-m/h-SOD1 on immunoblots of 100 μg of protein in detergent-soluble extracts from human frontal cortex (lanes 1), human hippocampus (lanes 2), human motor cortex (lanes 3), human spinal cord gray-matter (lanes 4) and white-matter (lanes 5) tracts. Proteins were stained with Coomassie blue (*E*) or immunoblotted with pAb-m/h-SOD1 (*D*).

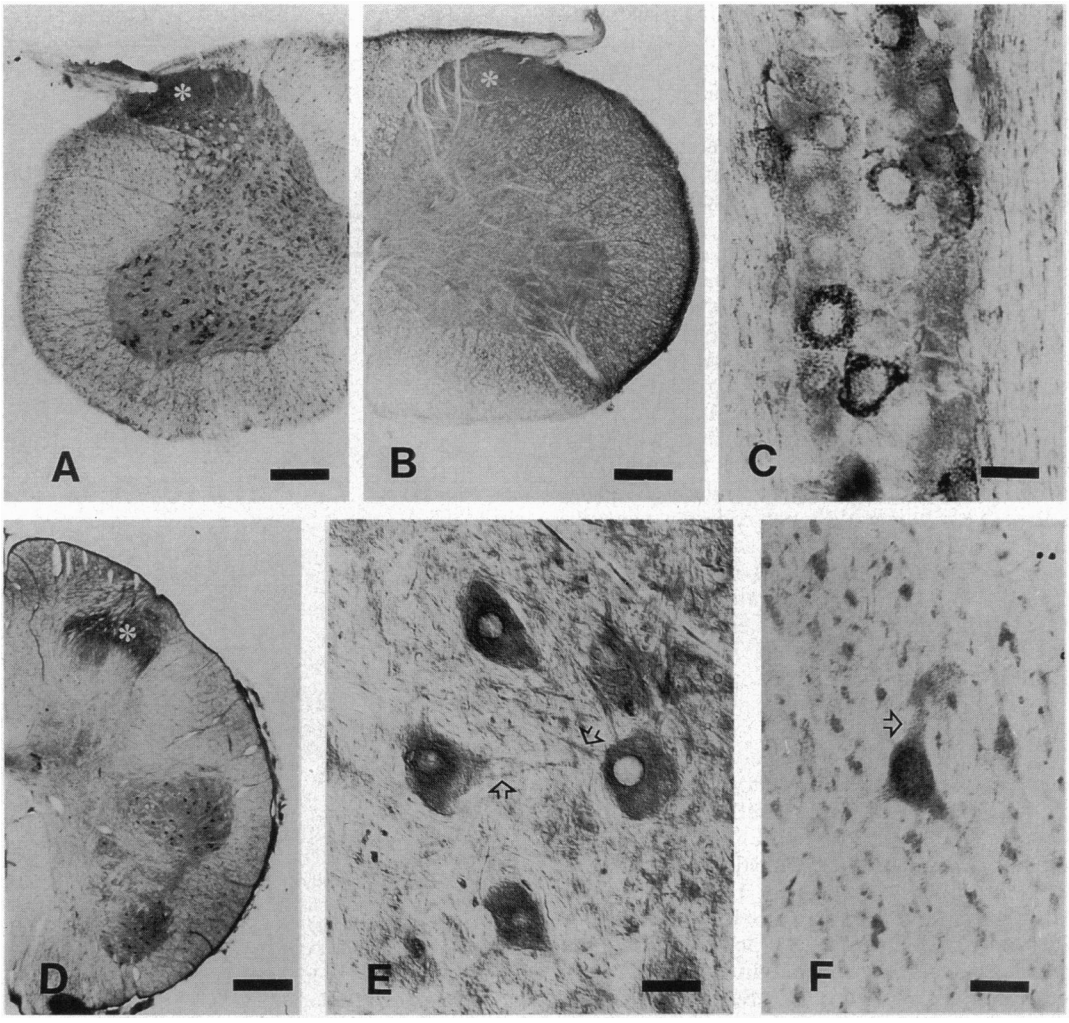

FIG. 2. Distribution of SOD1 in mammalian nervous tissue. (*A*) SOD1 distribution in mouse spinal cord shown by pAb-m/h-SOD1. Immunoreactivity is found in motor neurons, interneurons, and substantia gelatinosa (asterisk). (Bar = 220 μm.) (*B*) Adjacent section immunostained with pAb-m/h-SOD1 preadsorbed to the immunizing peptide. (Bar = 220 μm.) (*C*) Neurons of mouse trigeminal ganglion display strong immunostaining. Some axons are also highlighted by immunoreaction. (Bar = 45 μm.) (*D*) SOD1 distribution in human lumbar spinal cord. Asterisk indicates strong immunoreactivity in the substantia gelatinosa. (Bar = 1000 μm.) (*E*) High-magnification view of SOD1 immunoreactivity in motor neurons of human lumbar spinal cord (longitudinal section). Arrows point to dendrites that are immunoreactive. (Bar = 40 μm.) (*F*) SOD1 immunoreactivity in the perikaryon of a large pyramidal neuron from human motor cortex. Arrow points to basal dendrites that are immunostained. (Bar = 10 μm.)

(denoted by the asterisk in Fig. 2*A*), as well as motor neuron terminals in striated muscle (data not shown). These observations indicate that SOD1 is also present in terminals of some axons. Both motor and sensory cranial nuclei in the brainstem showed marked SOD1 immunoreactivity, with particular abundance in the nuclei of the III, V, VII, VIII, and IX cranial nerves. Dorsal root (data not shown) and trigeminal (Fig. 2*C*) ganglion cells were also immunoreactive.

In other regions of the brain, many neurons immunostained with pAb-m/h-SOD1 antibody, with particularly conspicuous reactivity in large and medium-size pyramidal neurons in the cortex, as well as subsets of neurons intensively stained in hippocampus, caudoputamen, globus pallidum, substantia nigra, and thalamus. In cerebral cortex, large and medium-size pyramidal neurons showed intense SOD1 staining (Fig. 3). As in motor neurons, particulate staining was seen throughout each perikaryon. Nonpyramidal neurons showed less immunoreactivity. The hippocampal formation showed a very distinctive distribution; neurons in sectors CA3 and CA4 of the stratum pyramidale were intensely stained for SOD1 (Fig. 3 *A* and *B*), whereas CA1 neurons showed much less immunoreactivity (Fig. 3*A*). Granular cells in the dentate gyrus were almost devoid of SOD1 immunoreactivity. In striatum, medium-size aspiny neurons were conspicuously immunoreactive, while other striatal neurons and the striosomal compartments were not immunostained. In thalamus, the anterodorsalis, reticularis, and ventralis nuclei exhibited prominent immunoreactive neurons. Neurons in the mitral cell layer of the olfactory bulb, pyriform cortex, amygdala complex, and red nuclei were also strongly immunostained (data not shown). In human (Fig. 2*F*) and nonhuman (Fig. 3 *C* and *D*) primates the patterns of immunoreactivity in cortex, subcortical nuclei, and brainstem nuclei were similar.

Immunoelectron Microscopic Localization of SOD1 in Axons, Dendrites, and Perikarya of Motor Neurons. To define the subcellular distributions of SOD1 within subcompartments of motor neurons, immunoelectron microscopy was used with pAb-m/h-SOD1 antibody and silver-enhanced immunogold techniques. Immunogold particles were present in the cytosol, preferentially in the perinuclear region and euchromatic areas in the nucleus (Fig. 4*A*). Mitochondria and other organelles did not stain. In motor neurons, clusters of immunogold particles were seen in the proximal portion of dendrites and in axonal compartments (Fig. 4 *C* and *D*). In white-matter tracts of the

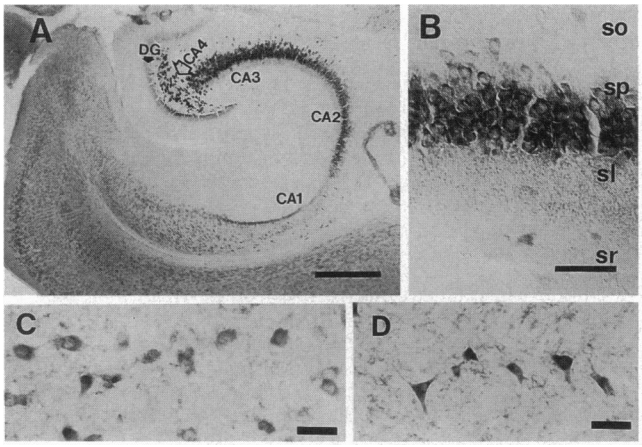

FIG. 3. SOD1 immunoreactivity in hippocampus. (*A*) Distribution of SOD1 immunoreactivity in the hippocampal formation of mouse. Note the enrichment of SOD1 in CA2, CA3, and CA4 sectors. (Bar = 700 μm.) (*B*) Detail of the CA3 sector of the hippocampus demonstrating the strong SOD1 immunoreactivity in the stratum pyramidale (sp) and punctiform immunostaining in the stratum lacunosum (sl). The stratum oriens (so) and stratum radiatum (sr) are devoid of SOD1 immunoreactivity. (Bar = 60 μm.) (*C* and *D*) SOD1 immunoreactivity in neurons of the substantia nigra (*C*) and globus pallidum (*D*) from baboon brain. (Bars = 45 μm.)

spinal cord, clusters of immunogold particles were often identified in cross sections of myelinated axons (Fig. 4*C*). Moreover, in some axons, immunogold particles were associated with membranous profiles morphologically similar to peroxisomes (Fig. 4*B*), organelles previously proposed to contain SOD1 (27). Similar subcellular patterns of SOD1 immunoreactivity were identified in other neuronal populations (e.g., pyramidal neurons in cortex and hippocampus; data not shown). Specificity of the immunogold reactivity was confirmed by the absence of immunogold particles in parallel analyses using pAb-m/h-SOD1 antibody preincubated with the immunizing peptide (data not shown).

DISCUSSION

Although SOD1 has been reported to be expressed in many different cells (1), examination of its distribution in the human or mouse nervous system has been limited to examination in the hippocampus (5, 6, 12) and the substantia nigra [by *in situ* hybrydization (7)]. Only a study in canine and rat brain has disclosed the extensive presence of SOD1 in various regions of the brain (8), but study of the spinal cord has not been reported. The current effort, which takes advantage of a new, highly specific anti-peptide antibody, demonstrates not only that SOD1 is a component of several classes of neurons but also that it is selectively enriched in a subset of neurons, particularly motor neurons in spinal cord and brainstem, pyramidal neurons in sectors CA2–CA4 of hippocampus, and neurons in neocortex, pyriform cortex, and amygdala. Much of the SOD1 immunoreactivity appears to be in the cytoplasm of perikarya, dendrites, and axons, with immunoreactivity also present in nuclei and in membranous organelles, presumably peroxisomes. As immunocytochemistry is not amenable to precise quantitation, we cannot be sure as to the proportion of

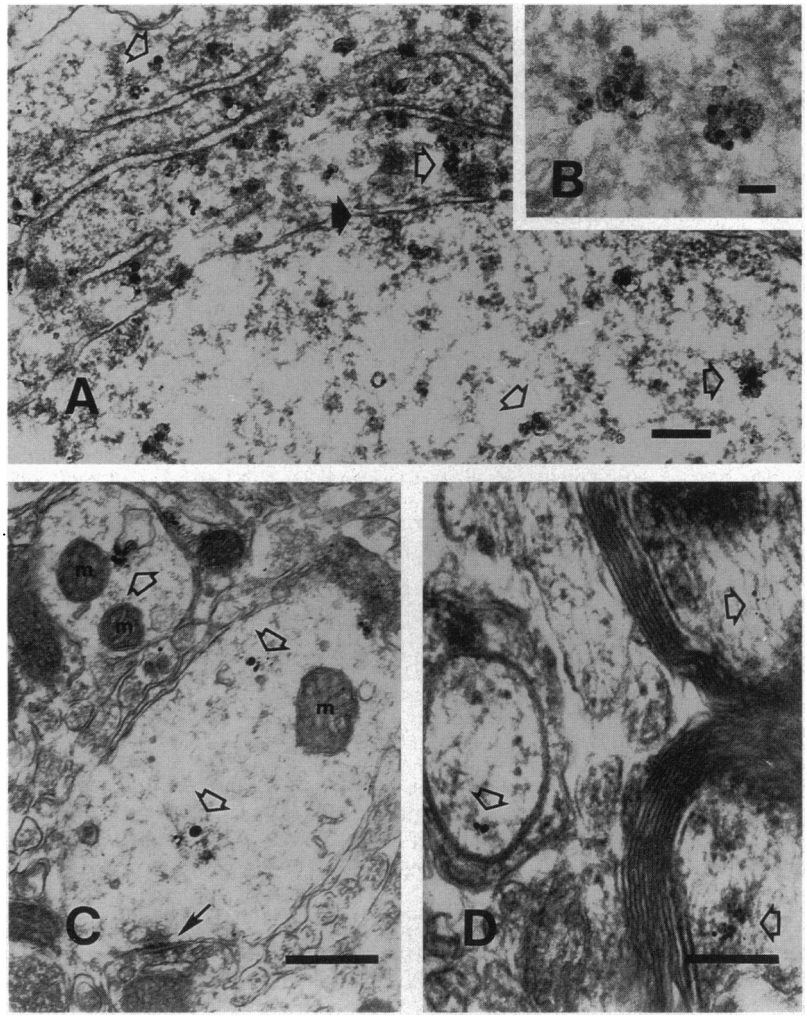

FIG. 4. Localization of SOD1 in neuronal perikarya, dendrites, and axons. Immunoelectron microscopy with pAb-m/h-SOD1 and silver-enhanced gold secondary antibodies was used to identify SOD1 in the perikarya (*A*), membranous organelles (*B*), dendrites (*C*), and axons (*D*) of mouse spinal cord (*A*, *B*, and *D*) and hippocampus (*C*). (*A*) Open arrows denote prominent staining in the perinuclear region. Clusters of particles are seen in the nucleus. Solid arrow indicates the nuclear membrane. (Bar = 0.25 μm.) (*B*) Clusters of immunogold particles on membranous organelles, presumably peroxisomes. (Bar = 0.10 μm.) (*C*) Open arrows point to immunogold particles in dendrites. Thin solid arrow points to a synapsis; mitochondria are denoted (m). (Bar = 0.25 μm.) (*D*) Cross section of two myelinated axons (at right) and on unmyelinated axon (at left) shows clusters of particles in the axonal compartment (open arrows). (Bar = 0.25 μm.)

SOD1 in each neuronal compartment, although the highest concentration appears to be in cell bodies (Fig. 2). However, since simple geometric considerations demonstrate that for large lumbar motor neurons in humans >99% of the cell volume is in the axon, a substantial portion of SOD1 is probably within axons.

Moreover, the presence of SOD1 in the axonal compartment strongly suggests that the enzyme is carried by anterograde transport, a conclusion further supported by accumulation of SOD1 at nerve termini (Fig. 2). Only a few astrocytes in white matter and scattered microglial cells appear to have significant amounts of SOD1. No comparative or topographic studies on the cellular distributions of SOD1 have been previously reported, but our results are in agreement with previous biochemical and immunocytochemical studies that suggest differential expression of SOD1 in different regions of the brain (4, 8) and with studies that have focused on the presence of SOD1 mRNA or protein in discrete populations of neurons (5–8).

Our immunocytochemical findings in human and primate hippocampus show some differences from previous studies that used *in situ* hybridization and immunocytochemistry to report similar levels in the distribution of SOD1 mRNA and protein in all regions of the cornu Ammonis and dentate gyrus (5, 12). We have no explanation to account for the discrepancies with previous reports. Our investigations demonstrate that neurons in the CA1 sector (Sommer's sector), known to be susceptible to hypoxic/ischemic injury (28, 29), have relatively low levels of SOD1 compared with the CA3 and CA4 sectors. It is possible that the limited amount of SOD1 in the CA1 region may contribute to the susceptibility of this neuronal population to ischemic or hypoxic insults.

With regard to the mechanisms whereby mutations in SOD1 cause FALS, our findings show no evident correlations between the apparent abundance of SOD1 immunoreactivity in various neuronal populations and the vulnerabilities of neuronal degeneration in ALS. The apparent abundance of SOD1 in motor neurons of spinal cord and brainstem, as well as other subsets of nerve cells, suggests an especially important role for this enzyme in the neuroprotective pathways in these neurons. However, still unsettled is the way in which SOD1 mutations alter the activity of the enzyme to cause neuronal dysfunction and death, as some FALS-linked SOD1 mutations retain full specific activity, while others seem completely inactive (30). Further, several lines of transgenic mice expressing the FALS-associated SOD1 mutants exhibit phenotypic and pathologic changes associated with ALS. In at least one line, the mutant enzyme is quite active (19), with disease ensuing despite higher SOD1 levels than in wild-type mice.

As to the cascade of events leading to motor neuron death, the sum of these previous findings strongly suggests that the FALS-associated SOD1 mutations lead, at least in some cases, to aberrant enzymes with gain of adverse property(ies). Our findings here further narrow the range of possible mechanisms of motor neuron death in two additional aspects. (*i*) Proof that SOD1 is an abundant component in perikarya, dendrites, and axons of motor neurons strongly suggests that defects arising from SOD1 mutations act within vulnerable neurons, rather than from SOD1 deficiencies/activities in cells that interact with motor neurons. (*ii*) Combining the apparent abundance of SOD1 in motor neurons with our discovery that distribution of SOD1 in other neurons does not parallel vulnerability to SOD1 mutation makes it implausible that disease results from a barely adequate level of SOD1 in normal motor neurons, with FALS-associated mutations reducing SOD1 activity below a threshold necessary for motor neuron health. Rather, degeneration of neurons that apparently contain among the highest levels of SOD1 within all cell compartments is consistent with SOD1 mutations leading to aberrant, gain-of-function activities, which may be unrelated to conversion of superoxide to hydrogen peroxide. In this view, motor neurons (and other large, neurofilament-rich axons, such as the largest class of sensory neurons) may be selectively vulnerable in motor neuron disease (31), not because SOD1 activity is limiting, but because it is so abundant.

We acknowledge helpful discussions with Drs. John W. Griffin, Lee J. Martin, Phil Wong, and Michael Lee. We thank Venette Nehus and Frank Barksdale for their technical support. This work has been supported by grants from the National Institutes of Health (to D.W.C. and D.L.P.). D.W.C. and D.L.P. are Jacob Javitz Neuroscience Investigators. C.A.P. was the recipient of a Fogarty International Center fellowship. Z.X. is the recipient of a postdoctoral fellowship from the Muscular Dystrophy Association.

1. Fridovich, I. (1986) *Adv. Enzymol. Relat. Areas Mol. Biol.* **58,** 61–97.
2. Yu, B. P. (1994) *Physiol. Rev.* **74,** 139–162.
3. Ciriolo, M. R., Fiskin, K., De Martino, A., Corasaniti, M. T., Nistico, G. & Rotilio, G. (1991) *Mech. Ageing Dev.* **61,** 287–297.
4. Semsei, I., Rao, G. & Richardson, A. (1991) *Mech. Ageing Dev.* **58,** 13–19.
5. Ceballos, I., Javoy-Agid, F., Hirsch, E. C., Dumas, S., Kamoun, P. P., Sinet, P. M. & Agid, Y. (1989) *Neurosci. Lett.* **105,** 41–46.
6. Ceballos, I., Javoy-Agid, F., Delacourte, A., Defossez, A., Lafon, M., Hirsch, E., Nicole, A., Sinet, P. M. & Agid, Y. (1991) *Free Radical Res. Commun.* **12–13,** 571–580.
7. Zhang, P., Damier, P., Hirsch, E. C., Agid, Y., Ceballos-Picot, I., Sinet, P. M., Nicole, A., Laurent, M. & Javoy-Agid, F. (1993) *Neuroscience* **55,** 167–175.
8. Thaete, L. G., Crouch, R. K., Nakagawa, F. & Spicer, S. (1986) *J. Neurocytol.* **15,** 337–343.
9. Werns, S. W. & Luchesi, B. R. (1990) *Trends Pharmacol. Sci.* **11,** 161–166.
10. Matsuyama, T., Michishita, H., Nakamura, H., Tsuchiyama, M., Shimizu, S., Watanabe, K. & Sugita, M. (1993) *J. Cereb. Blood Flow Metab.* **13,** 135–144.
11. Bowling, A. C., Schulz, J. B., Brown, R. H., Jr., & Beal, M. F. (1993) *J. Neurochem.* **61,** 2322–2325.
12. Delacourte, A., Defossez, A., Ceballos, I., Nicole, A. & Sinet, P. M. (1988) *Neurosci. Lett.* **92,** 247–253.
13. Perrin, R., Briancon, S., Jeandel, C., Artur, Y., Minn, A., Penin, F. & Siest, G. (1990) *Gerontology* **36,** 306–313.
14. Somerville, M. J., Percy, M. E., Bergeron, C., Yoong, L. K. K., Grima, E. A. & McLachlan, R. C. (1991) *Mol. Brain Res.* **9,** 1–8.
15. Zemlan, F. P., Thienhaus, O. J. & Bosmann, H. B. (1989) *Brain Res.* **476,** 160–162.
16. Deng, H.-X., Hentati, A., Tainer, J. A., Iqbal, Z., Cayabyab, A., *et al.* (1993) *Science* **261,** 1047–1051.
17. Robberecht, W., Sapp, P., Viaene, M. K., Rosen, D., McKenna-Yasek, D., Haines, J., Horvitz, R., Theys, P. & Brown, R., Jr. (1994) *J. Neurochem.* **62,** 384–387.
18. Rosen, D. R., Siddique, T., Patterson, D., Figlewicz, D. A., Sapp, P., *et al.* (1993) *Nature (London)* **362,** 59–62.
19. Gurney, M. E., Pu, H., Chiu, A. Y., Dal Canto, M. C., Polchow, C. Y., Alexander, D. D., Caliendo, J., Hentani, A., Kwon, Y. W., Deng, H.-X., Chen, W., Zhai, P., Sufit, R. L. & Siddique, T. (1994) *Science* **264,** 1772–1774.
20. Lopata, M. A. & Cleveland, D. W. (1987) *J. Cell Biol.* **105,** 1707–1720.
21. Laemmli, U. K. (1970) *Nature (London)* **227,** 680–685.
22. Chan, J., Aoki, C. & Pickel, V. M. (1990) *J. Neurosci. Methods* **33,** 113–127.
23. Sherman, L., Dafni, N., Lieman-Hurwitz, J. & Groner, Y. (1983) *Proc. Natl. Acad. Sci. USA* **80,** 5465–5469.
24. Ho, Y.-S. & Crapo, J. D. (1987) *Nucleic Acids Res.* **15,** 6746.
25. Bewley, G. C. (1988) *Nucleic Acids Res.* **16,** 2728.
26. Epstein, C. J., Avraham, K. B., Lovett, M., Smith, S., Elroy-Stein, O., Rotman, G., Bry, C. & Groner, Y. (1987) *Proc. Natl. Acad. Sci. USA* **84,** 8044–8048.
27. Keller, G.-A., Warner, T. G., Steimer, K. S. & Hallewell, R. A. (1991) *Proc. Natl. Acad. Sci. USA* **88,** 7381–7385.
28. Pulsinelli, W. A., Brierley, J. B. & Plum, F. (1982) *Ann. Neurol.* **11,** 491–498.
29. Collins, R. C., Dobkin, B. H. & Choi, D. W. (1989) *Ann. Intern. Med.* **110,** 992–1000.
30. Borschelt, D. R., Lee, M. K., Slunt, H. S., Guarnieri, M., Xu, Z.-S., Wong, P. C., Brown, R. H., Price, D. L., Sisodia, S. S. & Cleveland, D. W. (1994) *Proc. Natl. Acad. Sci.* **91,** 8292–8296.
31. Kawamura, Y., Dyck, P. J., Shimono, M., Okasaki, H., Tateishi, J. & Doi, H. (1981) *J. Neuropathol. Exp. Neurol.* **40,** 667–675.